Monodisperse Oligofluorenes Forming Glassy-Nematic Films for Polarized Blue Emission

Yanhou Geng,[†] Sean W. Culligan,[†] Anita Trajkovska,[†] Jason U. Wallace,[†] and Shaw H. Chen*[,†,‡]

Department of Chemical Engineering and Laboratory for Laser Energetics, Center for Optoelectronics and Imaging, University of Rochester, 240 East River Road, Rochester, New York 14623-1212

Received August 28, 2002. Revised Manuscript Received November 26, 2002

The first series of monodisperse glass-forming, nematic oligofluorenes was synthesized following a divergent−convergent approach. Both chain length and pendant structure were found to affect solid morphology and phase transition temperatures. With optimized structural parameters, a T_g close to 150 °C and a T_c beyond 375 °C were achieved. This material class is characterized by its ability to form monodomain glassy nematic films via spin-coating, thermal annealing at 10 to 20 °C above T_g for 15−30 min, and cooling to room temperature without encountering crystallization. The absorption and emission dichroic ratios of 80−90-nm-thick films increase from 7 to 17 with an increasing molecular aspect ratio, while the photoluminescence quantum yield varies erratically from 43 to 60%. Superior stability of emissive color and of emission dichroic ratio and that against thermally activated crystallization were also demonstrated through prolonged heating of a film at 10 °C above T_g under argon.

I. Introduction

Organic materials with an extended π-conjugation have been intensely pursued for electronics, photonics, and optoelectronics over the past 2 decades.[1,2] The control of solid-state morphology via molecular design and material processing has become a critical issue from both the basic and applied perspectives. Specifically, the ability to accomplish uniaxial molecular alignment across a large area is crucial to technological advances, such as polarized light-emitting diodes[3,4] and thin film transistors.[5,6] While the feasibility of various approaches to uniaxial alignment has been demonstrated,[7−14] the one based on nematic mesomorphism, originating in molecular self-assembly, appears to be the most promising in terms of implementation and process scale-up. To reduce this concept to practice, π-conjugated nematic liquid crystals that are capable of preserving molecular alignment in the solid state upon cooling while bypassing crystallization are highly desirable. In principle, nematic-type thermotropic conjugated polymers could serve this particular purpose. Of all the conjugated polymers reported to date, polyfluorenes have emerged as a prime candidate. Optimization of macromolecular structure has also been attempted with respect to pendant structure and aspect ratio (relative to the persistence length) to maximize dichroic ratio and to avoid crystallization.[4,12] Such endeavors would be fruitful if polyfluorene structures were well-defined in terms of chain length, persistence length, and monomer sequence (in the case of copolymers).

Monodisperse conjugated oligomers are characterized by structural uniformity and regularity, chemical purity, solubility, and ease of processing into well-aligned films. These features facilitate systematic investigations of structure−property relationships that contribute to fundamental understanding and practical application. However, oligomers are generally less prone to glass transition than polymers. In addition, oligomers tend

* To whom correspondence should be addressed. E-mail: shch@lle.rochester.edu.
[†] Department of Chemical Engineering.
[‡] Laboratory for Laser Energetics.

(1) *Semiconducting Polymers: Chemistry, Physics and Engineering*; Hadziioannou, G., van Hutten, P. F., Eds.; Wiley-VCH: Weinheim, 2000.
(2) Müllen, K.; Wegner, G. *Electronic Materials: The Oligomer Approach*; Wiley-VCH: Weinheim, 1998.
(3) Grell, M.; Bradley, D. D. C. *Adv. Mater.* **1999**, *11*, 895, and references therein.
(4) (a) Neher, D. *Macromol. Rapid Commun.* **2001**, *22*, 1365. (b) Scherf, U.; List, E. J. W. *Adv. Mater.* **2002**, *14*, 477, and references therein.
(5) Sirringhaus, H.; Wilson, R. J.; Friend, R. H.; Inbasekaran, M.; Wu, W.; Woo, E. P.; Grell, M.; Bradley, D. D. C. *Appl. Phys. Lett.* **2000**, *77*, 406.
(6) Dimitrakopoulos, C. D.; Malenfant, P. R. L. *Adv. Mater.* **2002**, *14*, 99.
(7) Era, M.; Tsutsui, T.; Saito, S. *Appl. Phys. Lett.* **1995**, *67*, 2436.
(8) Sariciftci, N. S.; Lemmer, U.; Vacar, D.; Heeger, A. J.; Janssen, R. A. J. *Adv. Mater.* **1996**, *8*, 651.
(9) Cimrová, V.; Remmers, M.; Neher, D.; Wegner, G. *Adv. Mater.* **1996**, *8*, 146.
(10) Weder, C.; Sarwa, C.; Montali, A.; Bastiaansen, C.; Smith, P. *Science* **1998**, *279*, 835.
(11) Jandke, M.; Strohriegl, P.; Gmeiner, J.; Brütting, W.; Schwoerer, M. *Adv. Mater.* **1999**, *11*, 1518.
(12) (a) Grell, M.; Knoll, W.; Lupo, D.; Meisel, A.; Miteva, T.; Neher, D.; Nothofer, H.-G.; Scherf, U.; Yasuda, A. *Adv. Mater.* **1999**, *11*, 671. (b) Miteva, T.; Meisel, A.; Knoll, W.; Nothofer, H. G.; Scherf, U.; Müller, D. C.; Meerholz, K.; Yasuda, A.; Neher, D. *Adv. Mater.* **2001**, *13*, 565.
(13) (a) Grell M.; Bradley, D. D. C.; Inbasekaran, M.; Woo, E. P. *Adv. Mater.* **1997**, *9*, 798. (b) Whitehead, K. S.; Grell, M.; Bradley, D. D. C.; Jandke, M.; Strohriegl, P. *Appl. Phys. Lett.* **2000**, *76*, 2946.
(14) Contoret, A. E. A.; Farrar, S. R.; Jackson, P. O.; Khan, S. M.; May, L.; O'Neil, M.; Nicholls, J. E.; Kelly, S. M.; Richards, G. J. *Adv. Mater.* **2000**, *12*, 971.

10.1021/cm0208859 CCC: $25.00 © 2003 American Chemical Society
Published on Web 01/04/2003

Chart 1. Structures of Monodisperse Oligofluorenes

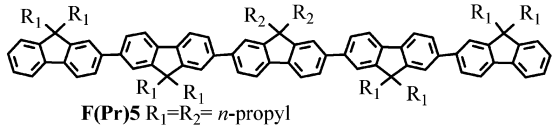

F(Pr)5 R_1=R_2= *n*-propyl
F(Pe)5 R_1=R_2= *n*-pentyl
F(MB)5 R_1=R_2=2-methybutyl
F(Pr)4F(EH)1 R_1= *n*-propyl, R_2=2-ethylhexyl
F(MB)4F(Pr)1 R_1=2-methylbutyl, R_2= *n*-propyl

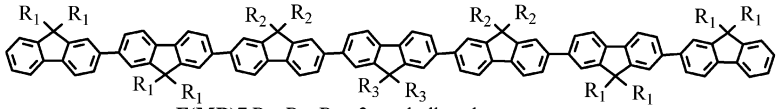

F(MB)7 R_1=R_2=R_3= 2-methylbutyl
F(Pr)5F(MB)2 R_1=R_3= *n*-propyl, R_2=2-methybutyl
F(Pr)5F(EH)2 R_1=R_3= *n*-propyl, R_2=2-ethylhexyl
F(MB)6F(EH)1 R_1=R_2= 2-methylbutyl, R_3=2-ethylhexyl

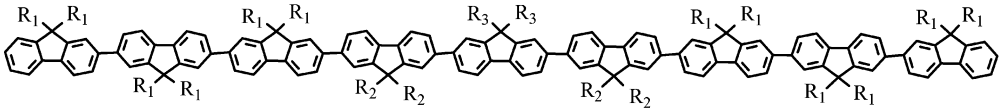

F(MB)9 R_1=R_2=R_3= 2-methylbutyl
F(MB)8F(EH)1 R_1=R_2= 2-methybutyl, R_3=2-ethylhexyl
F(MB)7F(EH)2 R_1=R_3= 2-methybutyl, R_2=2-ethylhexyl
F(MB)7F(DMO)2 R_1=R_3= 2-methylbutyl, R_2=3,7-dimethyloctyl

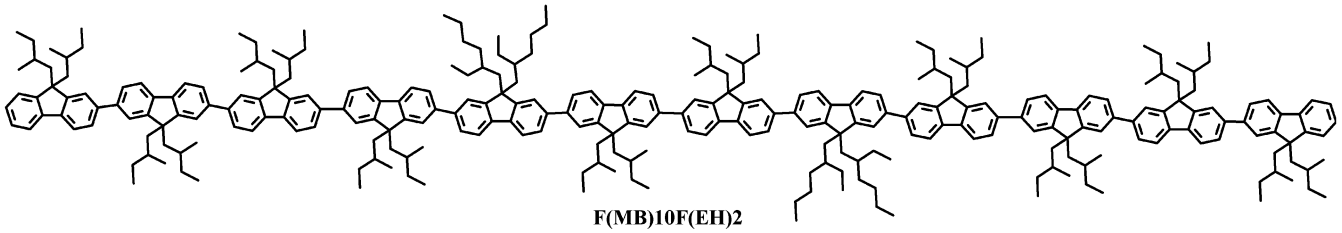

F(MB)10F(EH)2

to possess a low glass transition temperature if they manage to vitrify, which limits their practical utility. In fact, there exist few known examples of mesomorphic conjugated oligomers in the literature: a nematic oligo(*p*-phenylenevinylene) that readily crystallizes on cooling,[15] an oligotriacetylene that exhibits an unidentified mesophase,[16] and a smectic sexithiophene.[17] Furthermore, there is no evidence that these conjugated oligomers are capable of vitrification into macroscopically ordered solid films. Monodisperse oligofluorenes have been reported together with absorption and fluorescence maxima in dilute solution.[18] In a recent paper,[19] we have introduced one example each of glassy cholesteric and nematic oligofluorenes with an elevated glass transition temperature and a broad mesomorphic fluid temperature range, thus holding promise for electronics and photonics.

The present study was motivated by the following objectives: (1) to design and synthesize a series of readily soluble, monodisperse oligofluorenes with racemic aliphatic pendants capable of forming monodomain glassy nematic films with elevated transition temperatures T_g and T_c for linearly polarized blue emission; (2) to investigate the effects of chain length and pendant structure on thermotropic properties, phase transition temperatures, absorption and emission dichroism; and (3) to appraise photoluminescence quantum yield, and the temporal stability of film morphology, emissive color, and polarization ratio.

II. Results and Discussion

Chart 1 depicts the structures of monodisperse oligofluorenes that were synthesized as part of the present work following the divergent−convergent approach[19−21] (see Supporting Information). Specifically, penta-, hepta, and nonafluorenes were prepared by the Suzuki coupling reaction[22] in a 28−80% yield, whereas dodecafluorene was synthesized by the Yamamoto coupling reaction[23] in a 71% yield. Chemical purity and molecular structures of all the oligofluorenes were validated with elemental analysis in addition to the ^{1}H NMR and MALD/I-TOF-MS spectroscopic techniques.

Thermotropic properties as characterized by differential scanning calorimetry and polarizing optical

(15) Gill, R. E.; Meetsma, A.; Hadziioannou, G. *Adv. Mater.* **1996**, *8*, 212.
(16) Nierengarten, J.-F.; Guillon, D.; Heinrich, B.; Nicoud, J.-F. *Chem. Commun.* **1997**, 1233.
(17) Schenning, A. P. H. J.; Kilbinger, A. F. M.; Biscarini, F.; Cavallini, M.; Cooper, H. J.; Derrick, P. J.; Feast, W. J.; Lazzaroni, R.; Leclère, Ph.; McDonell, L. A.; Meijer, E. W.; Meskers, S. C. J. *J. Am. Chem. Soc.* **2002**, *124*, 1269.
(18) Klärner, G.; Miller, R. D. *Macromolecules* **1998**, *31*, 2007.
(19) Geng, Y. H.; Trajkovska, A.; Katsis, D.; Ou, J. J.; Culligan, S. W.; Chen, S. H. *J. Am. Chem. Soc.* **2002**, *124*, 8337.
(20) (a) Pearson, D. L.; Tour, J. M. *J. Org. Chem.* **1997**, *62*, 1376. (b) Pearson, D. L.; Tour, J. M. *J. Org. Chem.* **1997**, *62*, 1388.
(21) (a) Hensel, V.; Schlüter, A. D. *Chem.-Eur. J.* **1999**, *5*, 421. (b) Liess, P.; Hensel, V.; Schlüter, A. D. *Liebigs Ann. Chem.* **1996**, 1037.
(22) Miyaura, N.; Suzuki, A. *Chem. Rev.* **1995**, *95*, 2457.
(23) Yamamoto, T.; Morita, A.; Miyazaki, Y.; Maruyama, T.; Wakayama, H.; Zhou, Z.-H.; Makamura, Y.; Kanbara, T.; Sasaki, S.; Kubota, K. *Macromolecules* **1992**, *25*, 1214.

Table 1. Phase Transition Temperatures (T_g and T_c), Absorption, and Emission Dichroic Ratios (R_{abs} and R_{em}), Orientational Order Parameter (S_{abs}), and Photoluminescence Quantum Yield (Φ_{PL}) of Thermally Annealed, Spin-cast Films

compound	T_g,[a] °C	T_c,[a] °C	τ,[b] nm	R_{abs}[c]	S_{abs}[d]	R_{em}[c]	Φ_{PL},[e] %
			Pentamers				
F(Pr)5[f]	N/A	N/A	N/A	N/A	N/A	N/A	N/A
F(Pe)5[g]	72	N/A	N/A	N/A	N/A	N/A	N/A
F(MB)5	89	167	85	9.7 ± 0.4	0.74 ± 0.01	10.8 ± 0.5	54 ± 2
F(Pr)4F(EH)1[h]	112	178	N/A	N/A	N/A	N/A	N/A
F(MB)4F(Pr)1	84	124	88	7.1 ± 0.1	0.67 ± 0.01	6.9 ± 0.5	47 ± 6
			Heptamers				
F(Pr)5F(MB)2	149	366	81	15.5 ± 0.6	0.83 ± 0.01	14.1 ± 0.2	43 ± 4
F(Pr)5F(EH)2	116	319	78	10.8 ± 0.1	0.77 ± 0.01	10.5 ± 0.7	56 ± 4
F(MB)7[i]	110	320	N/A	N/A	N/A	N/A	N/A
F(MB)6F(EH)1	100	315	85	12.4 ± 0.1	0.77 ± 0.01	13.1 ± 0.7	60 ± 5
			Nonamers				
F(MB)9[j]	N/A	N/A	N/A	N/A	N/A	N/A	N/A
F(MB)8F(EH)1	115	>375	88	13.5 ± 0.4	0.81 ± 0.01	13.2 ± 1.5	59 ± 4
F(MB)7F(EH)2	109	>375	92	13.5 ± 0.2	0.81 ± 0.01	15.8 ± 0.8	54 ± 1
F(MB)7F(DMO)2	84	273	87	10.8 ± 0.4	0.77 ± 0.01	12.2 ± 0.4	57 ± 1
			Dodecamer				
F(MB)10F(EH)2	123	>375	90	16.7 ± 0.5	0.84 ± 0.01	17.2 ± 0.9	49 ± 1

[a] Transition temperatures gathered from DSC heating scans at 20 °C/min of samples preheated to 375 °C followed by cooling to −30 °C. T_g represents the inflection point across glass transition and T_c represents nematic to isotropic transition as identified by polarizing optical microscopy. [b] Spin-cast films of monodisperse oligofluorenes thermally annealed at 10−20 °C above T_g for 15−30 min to reach final values of R_{abs} and R_{em}; film thickness, τ, determined with spectroscopic ellipsometry. [c] R_{abs} evaluated at the absorption peak maximum and R_{em} at the higher-energy emission peak maximum of the two. [d] Orientational order parameter, $S_{abs} = (R_{abs} - 1)/(R_{abs} + 2)$. [e] Φ_{PL} determined following previously reported procedures.[19,25] [f] Heating scan showed crystalline melting at 318 °C and cooling scan at −20 °C/min showed crystallization at 267 °C; both scans revealed no mesomorphism under hot-stage polarizing optical microscopy. [g] Heating and cooling scans showed glass transition at 72 and 64 °C, respectively, without any mesomorphism. [h] Thin films showed crystal nuclei in addition to mesophase formation upon annealing. [i] Smectic A was observed above T_g (at 110 °C) followed by a transition to nematic mesomorphism at 150 °C and a T_c at 320 °C, thus preventing the preparation of a glassy nematic film. [j] Heating scan showed crystalline melting to a nematic fluid at 260 °C and cooling scan showed crystallization of a nematic fluid at 160 °C; both scans revealed no glass transition.

microscopy are summarized in Table 1. For these two types of analysis, samples were preheated to 375 °C, the upper temperature limit to avoid thermal decomposition. It was found that a minimum of five fluorene units and functionalization at the fluorene unit's C-9 position with appropriate aliphatic residues are essential to both glass transition and nematic mesomorphism. For instance, **F(Pr)5** and **F(Pe)5** are nonmesogenic, showing a crystalline melting point, T_m, at 318 °C and a glass transition temperature, T_g, at 72 °C, respectively. In contrast, **F(MB)5** exhibits a T_g at 89 °C and a nematic-to-isotropic transition temperature, T_c, at 167 °C, desirable features for realizing glassy nematic films. A comparison of **F(MB)5** with **F(Pe)5** suggests the benefit from branching aliphatic pendants in terms of mesophase formation. The nematic threaded textures, as shown in Figure 1a, were observed under hot-stage polarizing optical microscopy of a micrometer-thick film on a glass slide with a cover slip. Crystalline and nonmesogenic **F(Pr)5** is made glassy nematic with a T_g = 112 °C and a T_c = 178 °C by replacing the *n*-propyl pendants to the central fluorene unit with 2-ethylhexyl groups, that is, **F(Pr)4F(EH)1**. On the other hand, replacing 2-methylbutyl pendants to the central repeat unit of **F(MB)5** with *n*-propyl groups, that is, **F(MB)4F(Pr)1**, results in a depression in T_g and T_c by 5 and 43 °C, respectively. These emerging empirical rules governing structure−property relationships served to design higher oligomers with an objective of arriving at materials that are soluble and capable of forming stable glassy nematic films.

In the case of heptamers, all the co-oligomers are nematic fluids across an extended temperature range between T_g and T_c. In general, shorter pendants contribute to higher transition temperatures, with **F(Pr)5F(MB)2** exhibiting the highest values, T_g = 149 °C and T_c = 366 °C. However, homo-heptamer **F(MB)7** exhibits smectic A mesomorphism between 110 °C (i.e., T_g) and 150 °C, where a transition to nematic mesomorphism occurs. The more complex thermotropic behavior has apparently prevented the preservation of nematic mesomorphism in a glassy film via thermal annealing with subsequent cooling. To complete the series of higher oligomers, it is noted that, at an increasing chain length, bulkier aliphatic pendants are conducive to solubility, glass transition while bypassing crystallization, and nematic mesomorphism. Specifically, **F(MB)9** was found to undergo a crystalline-to-nematic transition at 260 °C on heating and a nematic-to-crystal transition at 160 °C on cooling, both executed at 20 °C/min. All the co-nonamers are nematic fluids beyond T_g ranging from 84 to 115 °C depending on the pendant structure. As in the case of co-dodecamer **F(MB)10F(EH)2** with a T_g at 123 °C, nematic mesomorphism exhibited by **F(MB)8F(EH)1** and **F(MB)7F(EH)2** was found to persist beyond 375 °C. Therefore, a molecular design strategy has been successfully formulated for glassy nematic oligofluorenes with elevated transition temperatures.

A thin film was prepared via spin-coating from a 1 wt % chloroform solution onto an alignment-coated and buffed fused silica substrate. Vacuum drying at room temperature overnight produced a pristine film that was subsequently annealed under argon at a temperature 10−20 °C above T_g for 15−30 min. A glassy nematic film was then obtained by cooling to room temperature while preserving the uniaxial molecular alignment mediated by nematic mesomorphism in the fluid state. The annealing time was dictated by the achievement of final

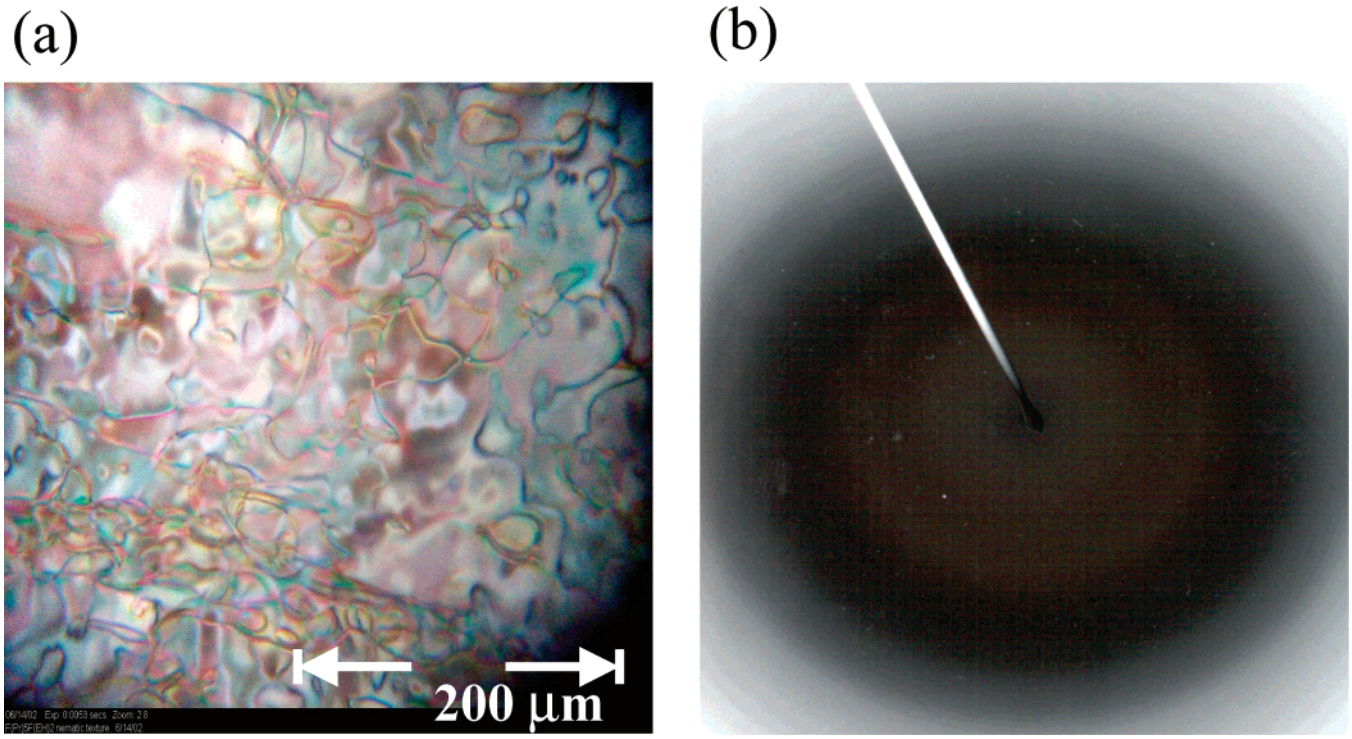

Figure 1. Micrographs of monodisperse glass-forming nematic oligofluorenes illustrated with **F(Pr)5F(MB)2**: (a) Nematic threaded textures observed under hot-stage polarizing optical microscopy of a micrometer-thick film on a microscope glass slide with a cover slip; (b) electron diffraction pattern of a spin-cast film to show the absence of crystallinity before and after thermal annealing.

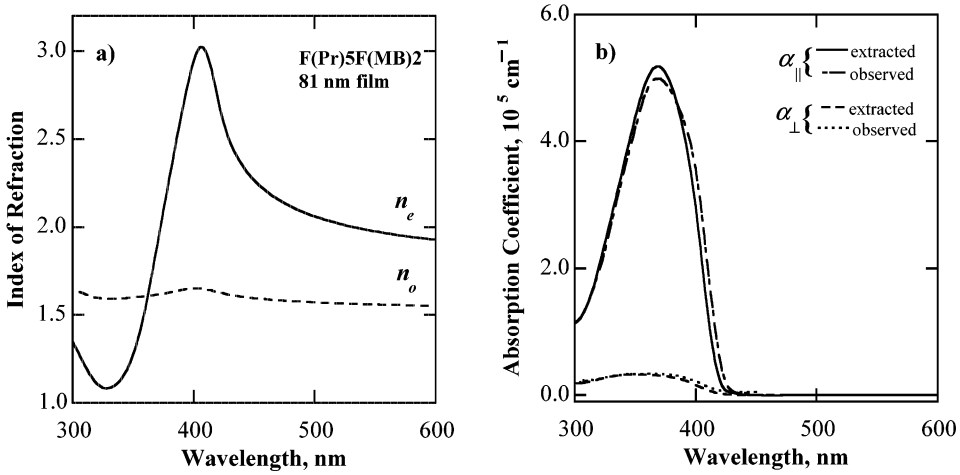

Figure 2. Ellipsometric characterization of an 81-nm-thick, thermally annealed film of **F(Pr)5F(MB)2**: (a) Extraordinary, n_e, and ordinary, n_o, refractive indices used for the determination of photoluminescence quantum yield and (b) anisotropic absorption coefficients parallel, $\alpha_{||}$, and perpendicular, $\alpha_{\perp}$, to the nematic director; the curves extracted from the ellipsometric analysis agree quite well with those independently measured with UV−vis−NIR spectrophotometry.

values of absorption and emission (with unpolarized excitation at 370 nm) dichroic ratios, $R_{abs} \equiv A_{||}/A_{\perp}$ and $R_{em} \equiv I_{||}/I_{\perp}$, in which A and I represent absorbance and emission intensity, respectively, and subscripts || and ⊥ specify directions parallel and perpendicular to the nematic director defined by substrate buffing. The resultant monodomain glassy nematic film is textureless under polarizing optical microscopy; moreover, electron diffraction reproduced in Figure 1b supports the absence of crystallinity. Spectroscopic ellipsometry[24] was employed to determine film thickness, ordinary and extraordinary refractive indices, n_o and n_e, and anisotropic absorption coefficients (i.e., absorbance per unit thickness) $\alpha_{||}$ and $\alpha_{\perp}$. Films were treated as optically biaxial, and the results indicated a uniaxial alignment since the refractive index normal to film was found to be identical to the ordinary in-plane refractive index. Both sets of extracted data are presented in Figure 2 for **F(Pr)5F(MB)2** as an example. The anisotropic refractive indices displayed in Figure 2a were used for the determination of photoluminescence quantum yield following the previously described procedures.[19,25] Figure 2b also reveals the agreement between the extracted anisotropic ab-

(24) Schubert, M.; Rheinländer, B.; Cramer, C.; Schmiedel, H.; Woollam, J. A.; Herzinger, C. M.; Johs, B. *J. Opt. Soc. Am. A* **1996**, *13*, 1930.

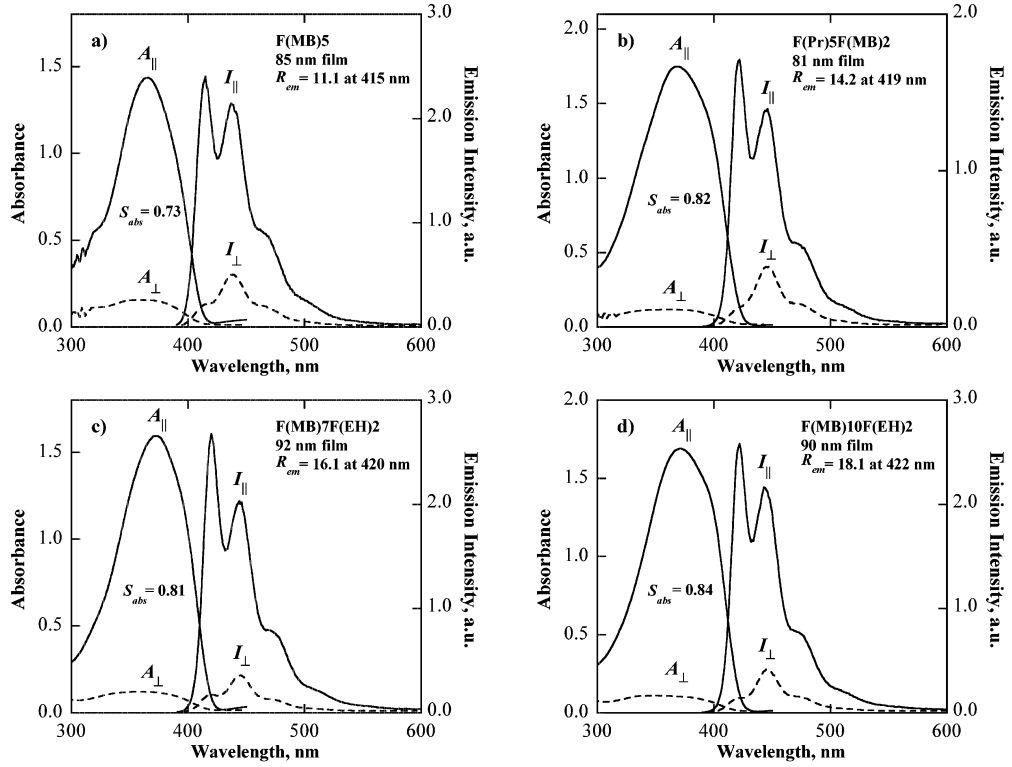

Figure 3. Linear dichroism and linearly polarized photoluminescence (with unpolarized excitation at 370 nm) of 80−90-nm-thick, thermally annealed films of (a) **F(MB)5**, (b) **F(Pr)5F(MB)2**, (c) **F(MB)7F(EH)2**, and (d) **F(MB)10F(EH)2** at an increasing emission dichroic ratio.

sorption coefficients and those calculated from an independent linear dichroism measurement of the same film using UV−vis−NIR spectrophotometry, thereby inspiring confidence in the ellipsometric technique.

One common feature of all the oligofluorenes reported here is their solubility in chloroform, methylene chloride, tetrahydrofuran, and toluene, which facilitates material synthesis, purification, and film processing by spin-coating. Pristine films' absorption spectra are somewhat broader than dilute solutions' (at 10^{-5} M fluorene units in chloroform) with approximately the same peak wavelengths (see Supporting Information). Furthermore, pristine films' emission spectra are similar to but red-shifted by up to 10 nm from dilute solutions', presumably due to emission from a more planar structure in the solid state. These results suggest an absence of aggregation in the ground or excited state. Anisotropic absorption and emission spectra are compiled for a penta-, hepta-, nona-, and dodecafluorene in Figure 3, where the values of film thickness, emission dichroic ratio, and the orientational order parameter based on absorption, $S_{abs} = (R_{abs} - 1)/(R_{abs} + 2)$, are also included. Note the increasing trend in R_{em} and S_{abs} with chain length for the given aliphatic pendants. Extensive results, including experimental uncertainties on the observed dichroic ratios and quantum yields for all glassy nematic films, are presented in Table 1 to offer the following observations. Regardless of chain length, co-oligomers are more favorable to the formation of morphologically stable glassy nematics than homooligomers. The insertion of bulky pendants tends to depress T_g and T_c of glassy nematics. Nonetheless, T_c generally increases with an increasing chain length. The absorption and emission dichroic ratios increase with molecular aspect ratio. The ease of forming a monodomain glassy nematic film is manifested as a superior orientational order parameter, $S_{abs} = 0.67-0.84$, achieved through thermal annealing under relatively mild conditions of temperature and time. The observed emission dichroic ratio of 17.2 ± 0.9 in a 90-nm film of **F(MB)10F(EH)2** compares favorably with the best performance data reported on photoluminescence of polyfluorene films.[13b,26] Within the series of monodisperse oligofluorenes, the photoluminescence quantum yield is by and large independent of chain length and pendant structure. Whitehead et al.[13b] reported that poly(dioctylfluorene) films yield an emission dichroic ratio of 10 and 25 from photoluminescence and electroluminescence, respectively. They attributed the observed difference to the fact that the recombination process is confined to the interfacial region in electroluminescence where the alignment is superior to the rest of the film. This is a factor that must be taken into consideration in the comparison of the two.

The effects of prolonged heating on light absorption and emission are illustrated in Figure 4 with a 92-nm-thick **F(MB)8F(EH)1** film. A typical electroluminescent device is encapsulated and could reach 90 °C at a relatively high forward bias.[27] The **F(MB)8F(EH)1** film's stability in terms of its morphology, emission

(25) Katsis, D.; Geng, Y. H., Ou, J. J.; Culligan, S. W.; Trajkovska, A.; Chen, S. H.; Rothberg, L. J. *Chem. Mater.* **2002**, *14*, 1332.

(26) Sainova, D.; Zen, A.; Nothofer, H.-G.; Asawapirom, U.; Scherf, U.; Hagan, R.; Bieringer, T.; Kostromine, S.; Neher, D. *Adv. Funct. Mater.* **2002**, *12*, 49.

(27) Zhou, X.; He, J.; Liao, L. S.; Lu, M.; Ding, X. M.; Hou, X. Y.; Zhang, X. M.; He, X. Q.; Lee, S. T. *Adv. Mater.* **2000**, *12*, 265.

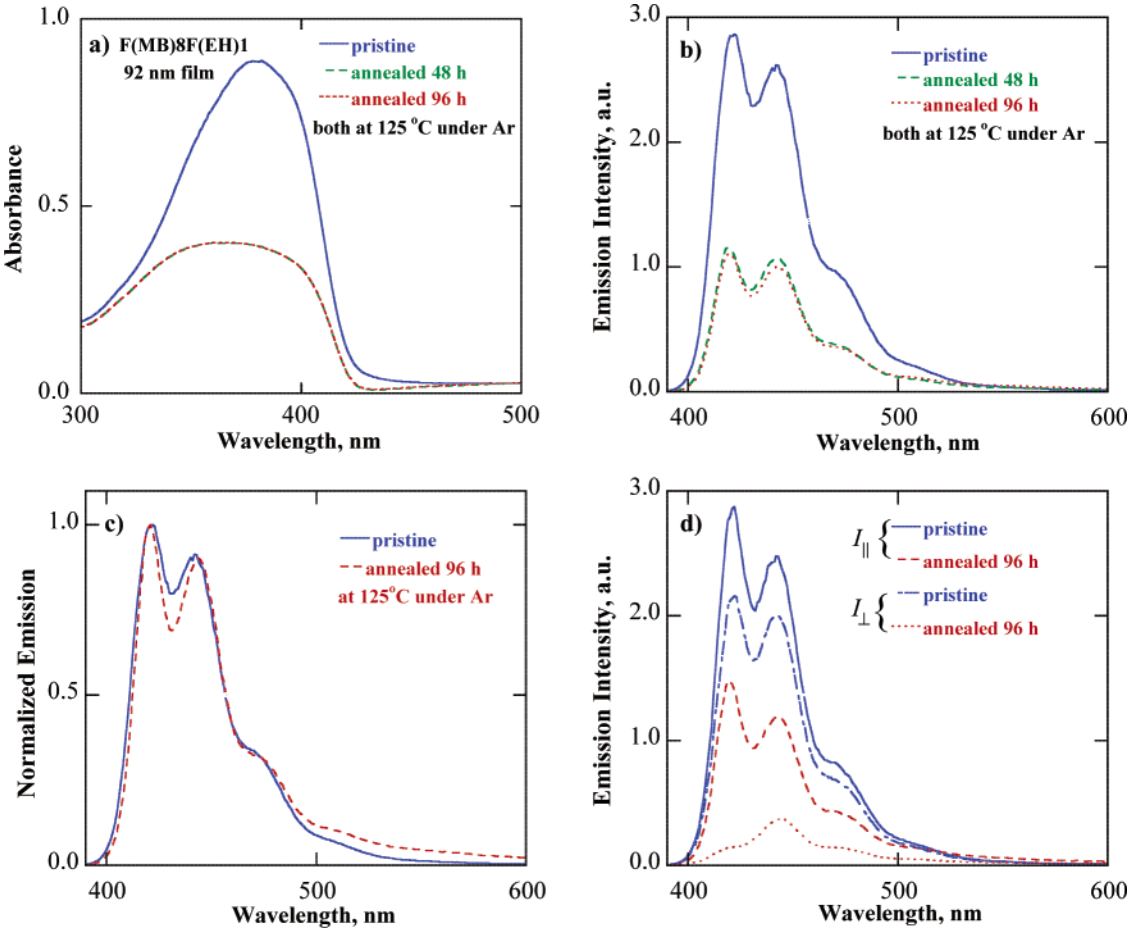

Figure 4. Effects of prolonged heating of a pristine, 92-nm-thick film of **F(MB)8F(EH)1** at 125 °C (i.e., 10 °C above T_g) under argon: (a) Hypochromism due to molecular alignment responsible for a reduction in absorbed photoexcitation at 370 nm by 30%; (b) accompanying reduction in integrated emission intensity; (c) stability of blue emission despite prolonged heating, and (d) increase in emission dichroic ratio at 420 nm from 1.3 to 11.9 as a result of annealing.

spectrum, and dichroic ratio was assessed by heating under argon at 10 °C above its T_g, namely, 125 °C. As shown in Figure 4a, thermal annealing up to 96 h resulted in hypochromism due to the increased interaction between π-orbitals.[28] A reduction in the absorbed photoexcitation at 370 nm by 30% plus some nonradiative decay paths caused by thermal treatment is responsible for a 55% decrease in the integrated emission intensity, as the emission spectrum of the annealed film is compared to that of the pristine film in Figure 4b. The normalized emission spectra of the pristine and the annealed film are compared in Figure 4c, which indicates the temporal stability of emissive color upon prolonged heating. Furthermore, polarization analysis of these emission spectra, as reported in Figure 4d, revealed that R_{em} at the higher energy emission peak (420 nm) increases from 1.3 (pristine film) to 11.9 (annealed film), a value consistent with that upon annealing of a pristine film for 15−30 min at the same temperature (see Table 1). A formerly annealed film left at room temperature in air for 3 months was found to retain its emissive color stability and dichroic ratio.

(28) Cantor, C. R.; Schimmel, P. R. *Biophysical Chemistry, Part II: Techniques for the Study of Biological Structure and Function*; W. H. Freeman and Company: New York, 1980.

III. Conclusions

In summary, the first series of monodisperse oligofluorenes with racemic pendants was synthesized following the divergent−convergent approach to furnish new insight into how chain length and pendant structure affect thermotropic and optical properties of spin-cast films. Thanks to the ease of processing into monodomain glassy nematic films, definitive information on structure−property relationships has emerged from experimental characterization using differential scanning calorimetry, polarizing optical microscopy, electron diffraction, linear dichroism, linearly polarized photoluminescence, and spectroscopic ellipsometry. Key observations are recapitulated as follows:

(1) In general, co-oligomers are more favorable than homo-oligomers, and branched aliphatic pendants are preferred over their linear counterparts as far as forming stable glassy nematics is concerned. Whereas T_g appears to be a function of both chain length and pendant structure, T_c tends to increase at an increasing chain length with pendant structure playing a secondary role.

(2) Through optimization with respect to chain length and pendant structure, oligofluorenes with a T_g up to 150 °C and a T_c beyond 375 °C have been realized. Monodomain glassy nematic films have resulted from

thermal annealing at 10−20 °C above T_g for up to 30 min with subsequent cooling to room temperature, indicating ease of material processing.

(3) A photoluminescence quantum yield of 43−60% has been achieved for blue emission with the resultant glassy nematic films. The absorption and emission dichroism was found to increase with an increasing molecular aspect ratio. The emission dichroic ratio evaluated at 17 in a 90-nm-thick dodecafluorene film compares favorably with the best performance reported to date.

(4) Heating a pristine nonafluorene film under argon at 125 °C for 96 h did not result in crystallization or a modification of its emissive color, whereas the loss in emission intensity was attributed to the diminished absorption of photoexcitation and some nonradiative decay paths. Moreover, the values of emission dichroic ratio were indistinguishable between 15 min and 96 h of heating.

IV. Experimental Section

Material Synthesis. All chemicals, reagents, and solvents were used as received from commercial sources without further purification except tetrahydrofuran (THF) and toluene that had been distilled over sodium/benzophenone and sodium, respectively. Synthesis of intermediates **11** and **20** has been reported elsewhere.[24] Synthesis of the rest of the intermediates is included in Supporting Information. The Suzuki and Yamamoto coupling reactions were employed for the preparation of all oligofluorenes.

General Procedure for the Synthesis of Oligofluorenes except Dodecafluorene by the Suzuki Coupling Reaction. Into a mixture of X−R−X (1 equiv), R′−Y (2.1 equiv), where R and R′ are fluorene segments and X and Y are halogen or boronate groups, and $Pd(PPh_3)_4$ (5 mol %) in a flask were added toluene and a 2.0 M aqueous solution of Na_2CO_3 (10 equiv; toluene:water = 10:6). The reaction mixture was stirred at 90 °C for 2 days. Methylene chloride was added upon cooling the reaction mixture. The organic layer was separated and washed with brine for drying over $MgSO_4$. Upon evaporating off the solvent, the residue was purified with column chromatography on silica gel except for **F(Pr)5**, which was recrystalized from chloroform.

Penta[9,9-bis(*n*-propyl)fluorene] (F(Pr)5). A light yellow solid was obtained in a 67% yield. ^{1}H NMR (400 MHz, $CDCl_3$): δ (ppm) 7.83−7.88 (m, 6H), 7.82 (d, J = 7.84 Hz, 2H), 7.78 (d, J = 7.47 Hz, 2H), 7.65−7.74 (m, 16H), 7.32−7.43 (m, 6H), 2.00−2.18 (m, 20H), 0.69−0.92 (m, 50H). Molecular weight calcd for $C_{95}H_{102}$: 1243.8. MALD/I TOF MS (dithranol) m/z ($[M]^+$): 1243.9. Anal. Calcd for $C_{95}H_{102}$: C, 91.73; H, 8.27. Found: C, 91.26; H, 8.27.

2,7-Bis[9,9,9′,9′-tetrakis(*n*-propyl)-2,2′-bifluoren-7-yl]-9,9-bis(2-ethylhexyl)fluorene (F(Pr)4F(EH)1). Eluent used for column chromatography was petroleum ether:chloroform (6:1). A light yellow solid was obtained in 80% yield. ^{1}H NMR (400 MHz, $CDCl_3$): δ (ppm) 7.83−7.87 (m, 6H), 7.81 (d, J = 7.84 Hz, 2H), 7.77 (dd, J = 6.52 Hz, 1.20 Hz, 2H), 7.65−7.72 (m, 16H), 7.32−7.43 (m, 6H), 2.00−2.18 (m, 20H), 0.69−1.02 (m, 70H). Molecular weight calcd for $C_{105}H_{122}$: 1384.1. MALD/I TOF MS (dithranol) m/z ($[M]^+$): 1384.0. Anal. Calcd for $C_{105}H_{122}$: C, 91.12; H, 8.88. Found: C, 91.24; H, 8.75.

Penta[9,9-bis(*n*-pentyl)fluorene] (F(Pe)5). Eluent used for column chromatography was petroleum ether:chloroform (8:1). A white solid was obtained in 41% yield. ^{1}H NMR (400 MHz, $CDCl_3$): δ (ppm) 7.84−7.89 (m, 6H), 7.83 (d, J = 7.85 Hz, 2H), 7.78 (d, J = 7.12 Hz, 2H), 7.65−7.75 (m, 16H), 7.32−7.42 (m, 6H), 2.02−2.18 (m, 20H), 1.05−1.22 (m, 40H), 0.65−0.90 (m, 50H). Molecular weight calcd for $C_{115}H_{142}$: 1524.4. MALD/I TOF MS (dithranol) m/z ($[M]^+$): 1524.0. Anal. Calcd for $C_{115}H_{142}$: C, 90.61; H, 9.39. Found: C, 90.70; H, 9.50.

2,7-Bis[9,9,9′,9′-tetrakis(2-methylbutyl)-2,2′-bifluoren-7-yl]-9,9-bis(*n*-propyl)fluorene (F(MB)4F(Pr)1). Eluent used for column chromatography was petroleum ether:chloroform (8:1). A white solid was obtained in 59% yield. ^{1}H NMR (400 MHz, $CDCl_3$): δ (ppm) 7.83−7.87 (m, 6H), 7.82(d, J = 8.10 Hz, 2H), 7.78 (d, J = 7.71 Hz, 2H), 7.62−7.74 (m, 16H), 7.29−7.48 (m, 6H), 1.90−2.30 (m, 20H), 0.53−1.06 (m, 58H), 0.32−0.44 (m, 24H). Molecular weight calcd for $C_{111}H_{134}$: 1468.3. MALD/I TOF MS (dithranol) m/z ($[M]^+$): 1467.9. Anal. Calcd for $C_{111}H_{134}$: C, 90.80; H, 9.20. Found: C, 90.51; H, 9.29.

Penta[9,9-bis(2-methylbutyl)fluorene] (F(MB)5). Eluent used for column chromatography was petroleum ether:chloroform (8:1). A white solid was obtained in 76% yield. ^{1}H NMR (400 MHz, $CDCl_3$): δ (ppm) 7.82−7.87 (m, 6H), 7.82 (d, J = 8.10 Hz, 2H), 7.77 (d, J = 7.35 Hz, 2H), 7.62−7.74 (m, 16H), 7.30−7.48 (m, 6H), 2.17−2.31 (m, 10H), 1.90−2.01 (m, 10H), 0.55−1.10 (m, 60H), 0.32−0.43 (m, 30H). Molecular weight calcd for $C_{115}H_{142}$: 1524.4. MALD/I TOF MS (dithranol) m/z ($[M]^+$): 1524.1. Anal. Calcd for $C_{115}H_{142}$: C, 90.61; H, 9.39. Found: C, 90.56; H, 9.31.

2,7-Bis[9,9-bis(2-methylbutyl)-9′,9′,9″,9″-tetrakis(*n*-propyl)-7,2′;7′,2″-terfluoren-2-yl]-9,9-bis(*n*-propyl)fluorene (F(Pr)5F(MB)2). Eluent used for column chromatography was petroleum ether:chloroform (6:1). A light yellow solid was obtained in 56% yield. ^{1}H NMR (400 MHz, $CDCl_3$): δ (ppm) 7.78−7.89 (m, 13H), 7.66−7.77 (m, 25H), 7.32−7.44 (m, 6H), 2.28−2.35 (m, 4H), 2.00−2.15 (m, 24H), 1.00−1.07 (m, 4H), 0.63−0.99 (m, 70H), 0.39−0.45 (m, 12H). Molecular weight calcd for $C_{141}H_{158}$: 1852.8. MALD/I TOF MS (dithranol) m/z ($[M]^+$): 1852.3. Anal. Calcd for $C_{141}H_{158}$: C, 91.40; H, 8.60. Found: C, 91.47; H, 8.51.

2,7-Bis[9,9-bis(2-ethylhexyl)-9′,9′,9″,9″-tetrakis(*n*-propyl)-7,2′;7′,2″-terfluoren-2-yl]-9,9-bis(*n*-propyl)fluorene (F(Pr)5F(EH)2). Eluent used for column chromatography was petroleum ether:chloroform (6:1). A light yellow solid was obtained in a 33% yield. ^{1}H NMR (400 MHz, $CDCl_3$): δ (ppm) 7.83−7.88 (m, 10H), 7.82 (d, J = 7.86 Hz, 2H), 7.77 (dd, J = 7.60 Hz, 0.96 Hz, 2H), 7.64−7.73 (m, 24 H), 7.33−7.43 (m, 6H), 2.01−2.19 (m, 28H), 0.61−0.99 (m, 110H). Molecular weight calcd for $C_{153}H_{182}$: 2021.1. MALD/I TOF MS (dithranol) m/z ($[M]^+$): 2020.5. Anal. Calcd for $C_{153}H_{182}$: C, 90.92; H, 9.08. Found: C, 90.64; H, 9.16.

Hepta[9,9-bis(2-methylbutyl)fluorene] (F(MB)7). Eluent used for column chromatography was petroleum ether:chloroform (5:1). A light yellow solid was obtained in 59% yield. ^{1}H NMR (400 MHz, $CDCl_3$): δ (ppm) 7.82−7.88 (m, 10H), 7.81 (d, J = 8.15 Hz, 2H), 7.77 (d, J = 7.38 Hz, 2H), 7.62−7.74 (m, 24H), 7.29−7.48 (m, 6H), 2.12−2.29 (m, 14H), 1.90−2.01 (m, 14H), 0.74−1.08 (m, 42H), 0.61−0.74 (m, 42H), 0.31−0.48 (m, 42H). Molecular weight calcd for $C_{161}H_{198}$: 2133.3. MALD/I TOF MS (dithranol) m/z ($[M]^+$): 2132.4. Anal. Calcd for $C_{161}H_{198}$: C, 90.65; H, 9.35. Found: C, 90.48; H, 9.49.

Nona[9,9-bis(2-methylbutyl)fluorene] (F(MB)9). Eluent used for column chromatography was petroleum ether:chloroform (4:1). A light yellow solid was obtained in a 45% yield. ^{1}H NMR (400 MHz, $CDCl_3$): δ (ppm) 7.83−7.88 (m, 14H), 7.82 (d, J = 8.16 Hz, 2H), 7.77 (d, J = 7.38 Hz, 2H), 7.62−7.74 (m, 32H), 7.29−7.44 (m, 6H), 1.89−2.08 (m, 18H), 2.12−2.38 (m, 18H), 0.58−1.12 (m, 108H), 0.31−0.48 (m, 54H). Molecular weight calcd for $C_{207}H_{254}$: 2742.3. MALD/I TOF MS (dithranol) m/z ($[M]^+$): 2741.7. Anal. Calcd for $C_{207}H_{254}$: C, 90.66; H, 9.34. Found: C, 90.61; H, 9.51.

2,7-Bis[9,9,9′,9′,9″,9″-hexakis(2-methylbutyl)-7,2′;7′,2″-terfluoren-2-yl]-9,9-bis(2-ethylhexyl)fluorene (F(MB)6F(EH)1). Eluent used for column chromatography was petroleum ether:chloroform (6:1). A light yellow solid was obtained in 54% yield. ^{1}H NMR (400 MHz, $CDCl_3$): δ (ppm) 7.83−7.88 (m, 10H), 7.82 (d, J = 8.20 Hz, 2H), 7.78 (d, J = 7.38 Hz, 2H), 7.62−7.75 (m, 24H), 7.29−7.46 (m, 6H), 1.91−2.33 (m, 28H), 0.58−1.18 (m, 102H), 0.28−0.45 (m, 36H). Molecular weight calcd for $C_{167}H_{210}$: 2217.5. MALD/I TOF MS (dithranol) m/z ($[M]^+$): 2216.5. Anal. Calcd for $C_{167}H_{210}$: C, 90.45; H, 9.55. Found: C, 90.41; H, 9.63.

2,7-Bis[9,9,9′,9′,9″,9″,9‴,9‴-octakis(2-methylbutyl)-7,2′;7′,2″;7″,2‴-tetrafluoren-2-yl]-9,9-bis(2-ethylhexyl)flu-

orene (F(MB)8F(EH)1). Eluent used for column chromatography was petroleum ether:chloroform (5:1). A light yellow solid was obtained in 39% yield. ^{1}H NMR (400 MHz, $CDCl_3$): δ (ppm) 7.83−7.88 (m, 14H), 7.82 (d, J = 8.23 Hz, 2H), 7.77 (d, J = 7.35 Hz, 2H), 7.62−7.74 (m, 32H), 7.29−7.45 (m, 6H), 1.91−2.35 (m, 36H), 0.58−1.18 (m, 126H), 0.27−0.45 (m, 48H). Molecular weight calcd for $C_{213}H_{266}$: 2826.5. MALD/I TOF MS (dithranol) m/z ($[M]^+$): 2825.5. Anal. Calcd for $C_{213}H_{266}$: C, 90.51; H, 9.49. Found: C, 90.40; H, 9.62.

2,7-Bis[9,9-bis(2-ethylhexyl)-9′,9′,9″,9″,9‴,9‴-hexakis-(2-methylbutyl)-7,2′;7′,2″;7″,2‴-tetrafluoren-2-yl]-9,9-bis-(2-methylbutyl)fluorene (F(MB)7F(EH)2). Eluent used for column chromatography was petroleum ether:chloroform (5:1). A light yellow solid was obtained in a 28% yield. ^{1}H NMR (400 MHz, $CDCl_3$): δ (ppm) 7.83−7.87 (m, 14H), 7.82 (d, J = 8.28 Hz, 2H), 7.77 (d, J = 7.41 Hz, 2H), 7.61−7.73 (m, 32H), 7.29−7.48 (m, 6H), 1.88−2.38 (m, 36H), 0.58−1.18 (m, 144H), 0.26−0.46 (m, 42H). Molecular weight calcd for $C_{219}H_{278}$: 2910.6. MALD/I TOF MS (dithranol) m/z ($[M]^+$): 2910.1. Anal. Calcd for $C_{219}H_{278}$: C, 90.37; H, 9.63. Found: C, 90.37; H, 9.49.

2,7-Bis[9,9-bis(3,7-dimethyloctyl)-9′,9′,9″,9″,9‴,9‴-hexakis(2-methylbutyl)-7,2′;7′,2″;7″,2‴-tetrafluoren-2-yl]-9,9-bis(2-methylbutyl)fluorene (F(MB)7F(DMO)2). Eluent used for column chromatography was petroleum ether:chloroform (5:1). A light yellow solid was obtained in 46% yield. ^{1}H NMR (400 MHz, $CDCl_3$): δ (ppm) 7.83−7.88 (m, 14H), 7.82 (d, J = 8.12 Hz, 2H), 7.62−7.79 (m, 34H), 7.30−7.48 (m, 6H), 1.88−2.38 (m, 36H), 1.42−1.53 (m, 4H), 0.62−1.32 (m, 156H), 0.31−0.46 (m, 42H). Molecular weight calcd for $C_{227}H_{294}$: 3022.8. MALD/I TOF MS (dithranol) m/z ($[M]^+$): 3022.0. Anal. Calcd for $C_{227}H_{294}$: C, 90.20; H, 9.80. Found: C, 90.21; H, 9.92.

2,7′-Bis[9,9-bis(2-ethylhexyl)-9′,9′,9″,9″,9‴,9‴,9⁗,9⁗-octakis(2-methylbutyl)-7,2′;7′,2″;7″,2‴;7‴,2⁗-pentafluoren-2-yl]-9,9,9′,9′-tetrakis(2-methylbutyl)-7,2′-bifluorene (F(MB)-10F(EH)2). A mixture of $Ni(COD)_2$ (0.405 g, 1.47 mmol), 2,2′-bipyridine (0.230 g, 1.47 mmol), 1,5-cyclooctadiene (0.160 g, 1.47 mmol) in a mixed solvent of anhydrous DMF (5.0 mL), and toluene (5.0 mL) was stirred at 80 °C for 30 min. With the addition of **19b** (1.00 g, 0.490 mmol) in toluene (10.0 mL), the reaction mixture was stirred at 80 °C for 2 days. While the reaction mixture was left to cool to room temperature, chloroform (100 mL) and 2.0 M HCl (100 mL) were added. The mixture was then thoroughly stirred until the organic phase became clear. The organic layer was separated and washed with brine for drying over $MgSO_4$. Upon evaporation of the solvent, the residue was purified with column chromatography on silica gel using petroleum ether:chloroform (3:1) as the eluent to yield **F(MB)10F(EH)2** (0.663 g, 71%) as a light yellow solid. ^{1}H NMR (400 MHz, $CDCl_3$): δ (ppm) 7.83−7.89 (m, 20H), 7.82 (d, J = 8.24 Hz, 2H), 7.77 (d, J = 7.40 Hz, 2H), 7.62−7.75 (m, 44H), 7.30−7.44 (m, 6H), 1.91−2.35 (m, 48H), 0.60−1.10 (m, 180H), 0.28−0.49 (m, 60H). Molecular weight calcd for $C_{288}H_{362}$: 3824.0. MALD/I TOF MS (dithranol) m/z ($[M]^+$): 3823.1. Anal. Calcd for $C_{288}H_{362}$: C, 90.46; H, 9.54. Found: C, 90.54; H, 9.78.

Molecular Structures, Morphology, and Thermal Transition Temperature. ^{1}H NMR spectra were acquired in $CDCl_3$ with an Avance-400 spectrometer (400 MHz). Elemental analysis was carried out by Quantitative Technologies, Inc. Molecular weights were measured with a TofSpec2E MALD/I TOF mass spectrometer (Micromass, Inc., UK). Thermal transition temperatures were determined by differential scanning calorimetry (Perkin-Elmer DSC-7) with a continuous N_2 purge at 20 mL/min. Samples were preheated to 375 °C followed by cooling at −20 °C/min to −30 °C before taking the reported second heating scans at 20 °C/min. Morphology and the nature of phase transition were characterized with a polarizing optical microscope (DMLM, Leica, FP90 central processor and FP82 hot stage, Mettler Toledo).

Absorption and Fluorescence Spectra in Dilute Solution. Dilute solutions of oligofluorenes in chloroform were prepared at a concentration of 10^{-5} M in fluorene units. Absorption spectra were gathered with an HP 8453E UV−vis−NIR diode array spectrophotometer. Fluorescence spectra were collected with a spectrofluorimeter (Quanta Master C-60SE, Photon Technology International) at an excitation wavelength of 370 nm in a 90° orientation.

Preparation and Characterization of Neat Films. Optically flat fused silica substrates (25.4-mm diameter × 3-mm thickness, transparent to 200 nm, Escoproducts) were coated with a thin film of a commercial polyimide alignment layer (Nissan SUNEVER) and uniaxially rubbed. Films were prepared by spin-coating from 1 wt % solutions in chloroform at 5000 rpm followed by drying in vacuo overnight. Films for electron diffraction (JEM 2000 EX, JEOL USA) were prepared following the same procedures except on single-crystalline sodium chloride substrates (13-mm diameter × 2-mm thickness, International Crystal Laboratories). These films were floated off in a trough filled with deionized water for mounting onto copper grids. Thermal annealing was performed in dry argon purged glassware at temperatures 10−20 °C above the glass transition for 15−30 min. Polarizing optical microscopy revealed that annealed thin films were defect-free under a magnification factor of 500.

Absorption and linear dichroism of monodomain glassy nematic films were characterized using a UV−vis−NIR spectrophotometer (Lambda-900, Perkin-Elmer) and linear polarizers (HNP′B, Polaroid). Photoluminescence spectra, with and without polarization analysis, were collected using the spectrofluorimeter with a liquid light guide directing an unpolarized excitation beam at 370 nm onto the sample film at normal incidence. Emitted light normal to the film surface was detected and analyzed. The linearly polarized photoluminescence was characterized by controlling the film's nematic director relative to the two linear polarizers before the detector. First, the film was oriented vertically for gathering its emission spectra with a polarizer placed vertically and horizontally. The procedure was repeated with a horizontal orientation of the film. The results from two film orientations were averaged to minimize error. Experimental error was further reduced by inserting another polarizer at 45° between the first polarizer and the detector for all measurements. Variable angle spectroscopic ellipsometry (J. A. Woollam, V-VASE) was used to determine anisotropic refractive indices and absorption coefficients as well as film thickness following the literature procedures.[24]

Acknowledgment. We thank D. Katsis, L. J. Rothberg, S. D. Jacobs, and K. L. Marshall at the University of Rochester and C. W. Tang of Eastman Kodak Company in Rochester, NY, for technical advice and helpful discussions. We also thank A. J. Hoteling of the Analytical Technology Division of Eastman Kodak Company for the MALD/I-TOF measurement and analysis. We are grateful for the financial support provided by the National Science Foundation under Grant CTS-0204827 and the Multidisciplinary University Research Initiative, administered by the Army Research Office under DAAD19-01-1-0676. Additional funding was provided by the Department of Energy Office of Inertial Confinement Fusion under Cooperative Agreement No. DE-FC03-92SF19460 with the Laboratory for Laser Energetics and the New York State Energy Research and Development Authority. The support of DOE does not constitute an endorsement by DOE of the views expressed in this article.

Supporting Information Available: Synthesis, purification, and characterization of all intermediates except **11** and **20**; reaction scheme for all monodisperse oligofluorenes; representative MALD/I-TOF mass spectra; pristine films' absorption and emission spectra compared to dilute solutions' (at 10^{-5} M fluorene units in chloroform) (PDF). This material is available free of charge via the Internet at http://pubs.acs.org.

CM0208859